chapter 13

The Gamma Camera: Basic Principles

Radionuclide imaging is the most important application of radioactivity in nuclear medicine. Radionuclide imaging laboratories are found in almost every hospital, performing hundreds and even thousands of imaging procedures per month in larger institutions.

In this chapter, we discuss briefly some general aspects of radionuclide imaging, and we describe the basic principles of the most widely used imaging device, the *gamma camera,* also known as the *Anger scintillation camera,* named after its inventor, Hal Anger (see Chapter 1, Section C and Fig. 1-3). The performance characteristics of this instrument are discussed in Chapter 14. The use of the gamma camera for tomographic imaging is described in Chapter 17.

A. GENERAL CONCEPTS OF RADIONUCLIDE IMAGING

The purpose of radionuclide imaging is to obtain a picture of the distribution of a radioactively labeled substance within the body after it has been administered (e.g., by intravenous injection) to a patient. This is accomplished by recording the emissions from the radioactivity with external radiation detectors placed at different locations outside the patient. The preferred emissions for this application are γ rays in the approximate energy range of 80 to 500 keV (or annihilation photons, 511 keV). Gamma rays of these energies are sufficiently penetrating in body tissues to be detected from deep-lying organs, can be stopped efficiently by dense scintillators, and are shielded adequately with reasonable thicknesses of lead (see Fig. 6-17—soft tissue has attenuation properties similar to water). Alpha particles and electrons (β particles, Auger and conversion electrons) are of little use for imaging because they cannot penetrate more than a few millimeters of tissue. Therefore they cannot escape from within the body and reach an external radiation detector, except from very superficial tissues. Bremsstrahlung (see Fig. 6-1) generated by electron emissions is more penetrating, but the intensity of this radiation generally is very weak.

Imaging system detectors must therefore have good detection efficiency for γ rays. It is also desirable that they have energy discrimination capability, so that γ rays that have lost positional information by Compton scattering within the body can be rejected based on their reduced energy (see Chapter 6, Section C.3). A sodium iodide [NaI(Tl)] scintillation detector (see Chapter 7, Section C) provides both of these features at a reasonable cost; for this reason it is currently the detector of choice for radionuclides with γ-ray emissions in the range of 80-300 keV.

The first attempts at radionuclide "imaging" occurred in the late 1940s. An array of radiation detectors was positioned on a matrix of measuring points around the head. Alternatively, a single detector was positioned manually for separate measurements at each point in the matrix. These devices were tedious to use and provided only very crude mappings of the distribution of radioactivity in the head (e.g., left-side versus right-side asymmetries).

A significant advance occurred in the early 1950s with the introduction of the rectilinear scanner by Benedict Cassen (see Fig. 1-2). With this instrument, the detector was scanned mechanically in a raster-like pattern over the area of interest. The image was a pattern of dots imprinted on a sheet of paper by a mechanical printer that followed the scanning motion of the detector, printing the dots as the γ rays were detected.

The principal disadvantage of the rectilinear scanner was its long imaging time (typically many minutes) because the image was formed by sequential measurements at many individual points within the imaged area. The first gamma-ray "camera" capable of recording at all points in the image at one time was described by Hal Anger in 1953. He used a pinhole aperture in a sheet of lead to project a γ-ray image of the radionuclide distribution onto a radiation detector composed of a NaI(Tl) screen and a sheet of x-ray film. The film was exposed by the scintillation light flashes generated by the γ rays in the NaI(Tl) screen. Unfortunately, this detection system (especially the film component) was so inefficient that hour-long exposures and therapeutic levels of administered radioactivity were needed to obtain satisfactory images.

In the late 1950s, Anger replaced the film-screen combination with a single, large-area, NaI(Tl) crystal and a photomultiplier (PM) tube assembly to greatly increase the detection efficiency of his "camera" concept. This instrument, the *Anger scintillation camera,*[1] or *gamma camera,* has been substantially refined and improved since that time. Although other ideas for nuclear-imaging instruments have come along since then, none, with the exception of modern positron emission tomography systems (see Chapter 18), has matched the gamma camera for a balance of image quality, detection efficiency, and ease of use in a hospital environment. The gamma camera has thus become the most widely used nuclear-imaging instrument for clinical applications.

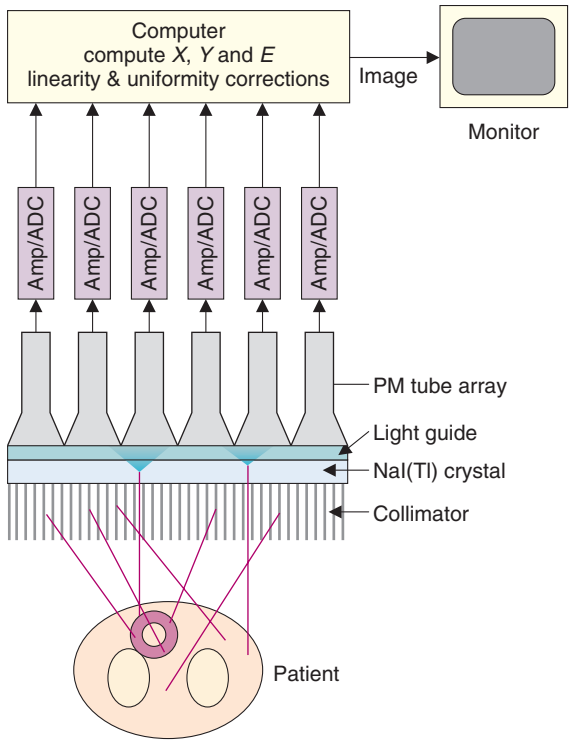

FIGURE 13-1 Basic principles and components of a modern gamma camera. The outputs of each photomultiplier (PM) tube are amplified and digitized using an analog-to-digital converter (ADC). The X-Y locations for each gamma ray that interacts in the NaI(Tl) crystal are computed from the digitized signals. The energy deposited by the gamma ray, *E*, which is proportional to the total measured pulse amplitude, also is computed by summing the individual PM tube signals. If *E* falls within the selected energy window, the event is accepted and placed at the appropriate X-Y location in the image.

B. BASIC PRINCIPLES OF THE GAMMA CAMERA

1. System Components

Figure 13-1 illustrates the basic principles of image formation with the gamma camera. The major components are a collimator, a large-area NaI(Tl) scintillation crystal, a light guide, and an array of PM tubes. Two features that differ from the conventional NaI(Tl) counting detectors described in Chapter 12 are crucial to image formation. The first is that an imaging *collimator* is used to define the direction of the detected γ rays. The collimator most commonly consists of a lead plate containing a large number of holes. By controlling which γ rays are accepted, the collimator forms a projected image of the γ-ray distribution on the surface of the NaI(Tl) crystal (see Section B.3). The second is that the NaI(Tl) crystal is viewed by an array of PM tubes, rather than a single PM tube. Signals from the PM tubes are fed to electronic or digital *position logic circuits,* which determine the X-Y location of each scintillation event, as it occurs, by using the weighted average of the PM tube signals (see Section B.2).

Individual events also are analyzed for energy, *E*, by summing the signals from all PM tubes. When the pulse amplitude of an event falls within the selected energy window, it is accepted and the *X* and *Y* values are binned into a discrete two-dimensional array of image elements, or *pixels.* An image is formed from a histogram of the number of events at each possible X-Y location. Large numbers of events are required to form an interpretable image because each pixel must

have a sufficient number of counts to achieve an acceptable signal-to-noise level. Because images often are formed in 64- × 64-pixel or 128- × 128-pixel arrays, the counting requirements are some 10^3 to 10^4 times higher than for a simple counting detector.

Images are displayed on a computer monitor, where image brightness and contrast may be manipulated and different color tables may be employed. More sophisticated digital image processing is discussed in Chapter 20.

Most modern gamma cameras are completely digital, in the sense that the output of each PM tube is directly digitized by an analog-to-digital converter (ADC). The calculation of X-Y position and pulse-height are performed in software based on the digitized PM tube signals, and errors in energy and positioning caused by noise and pulse distortions caused by the analog positioning circuitry are eliminated. This approach also permits improved handling of pulse pile-up at high counting rates, as described in Section B.2.

The gamma camera can be used for *static* imaging studies, in which an image of an unchanging radionuclide distribution can be recorded over an extended imaging time (e.g., minutes). Single contiguous images of the whole body can be obtained by scanning the gamma camera across the entire length of the patient. This can be achieved by moving either the bed or the gamma camera while adjusting the event positioning computation to account for this movement. Clinically important whole-body studies include bone scans of the skeleton, and the localization of tumors or their metastases in the body.

The gamma camera also can be used for *dynamic* imaging studies, in which changes in the radionuclide distribution can be observed, as rapidly as several images per second. This allows physiologic information to be obtained, such as the rate of tracer uptake or clearance from an organ of interest. Images also can be synchronized to electrocardiogram signals, permitting images of the heart in different phases of the cardiac cycle to be formed. These *gated* images can provide important information on cardiac function.

2. Detector System and Electronics

The gamma camera employs a single, large-area, rectangular NaI(Tl) detector crystal, usually 6- to 12.5-mm thick with sizes of up to 60 × 40 cm. Round crystals of 25 to 50 cm in diameter were used in many older systems. The NaI(Tl) crystal is surrounded by a highly reflective material such as TiO_2 to maximize light output and hermetically sealed inside a thin aluminum casing to protect it from moisture. An optical glass window on the back surface of the casing permits the scintillation light to reach the PM tubes. A cross section of a typical gamma camera crystal assembly is shown in Figure 13-2. The choice of thickness of the NaI(Tl) crystal is a trade-off between its detection efficiency (which increases with increasing thickness) and, as shown in Chapter 14, Section A.1, its intrinsic spatial resolution (which deteriorates with increasing thickness). Most general-purpose gamma cameras have crystal thicknesses of approximately 9.5 mm. For lower-energy γ emitters, such as ^{99m}Tc and ^{201}Tl, however, detection efficiency is adequate even with 6-mm-thick detector crystals.

An array of PM tubes is coupled optically to the back face of the crystal with a silicone-based adhesive or grease. Round PM tubes are arranged in a hexagonal pattern to maximize the area of the NaI(Tl) crystal that is covered. Some cameras use hexagonal (or rarely, square) cross-section PM tubes for better coverage of the NaI(Tl) crystal. Typical PM tube sizes are 5 cm in diameter. Most modern cameras employ between 30 and 100 PM tubes. Figure 13-3 shows a photograph of a 30-tube model. The PM tubes are encased in a thin magnetic shield (Chapter 7, Section C.2) to prevent changes in the gain caused by changes in the orientation of the gamma camera relative to the earth's magnetic field. The ultrasensitivity of PM tubes to magnetic fields also makes gamma cameras susceptible to the stray fields from magnetic resonance imaging systems.

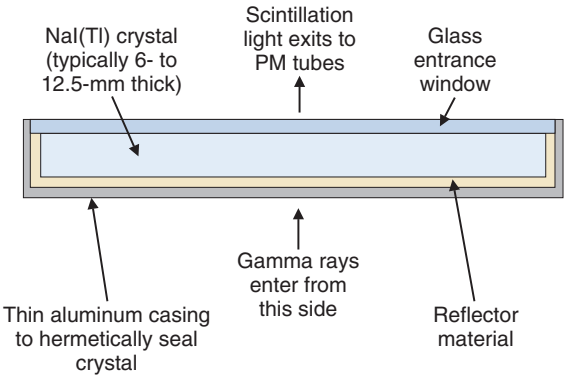

FIGURE 13-2 Schematic cross-section of a NaI(Tl) crystal assembly for a gamma camera.

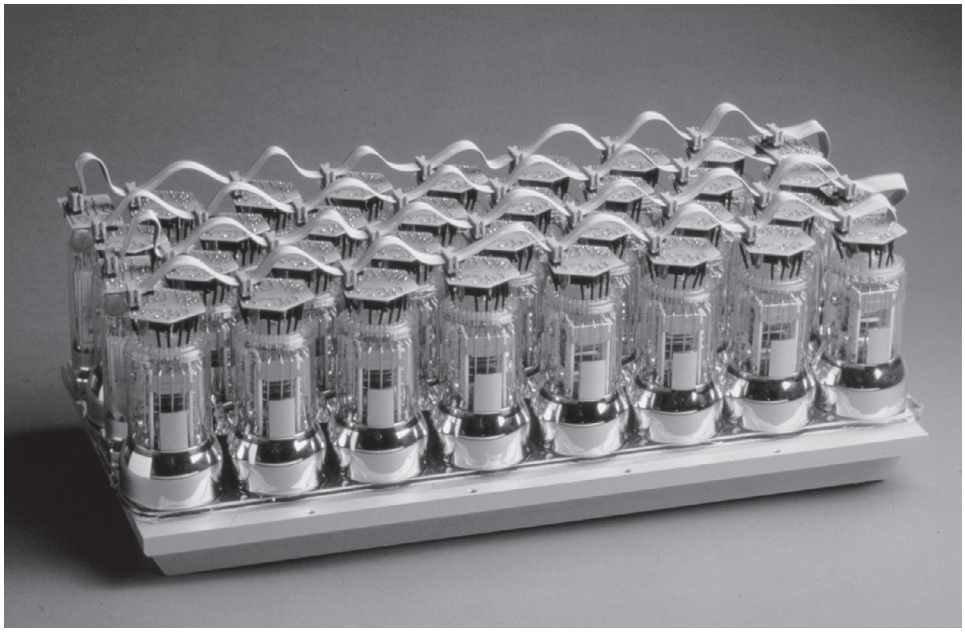

FIGURE 13-3 A rectangular gamma camera detector with the cover removed showing the photomultiplier (PM) tubes mounted on the NaI(Tl) crystal. In this example, the gamma camera detector measures 50 × 15 cm and is read out by 30 PM tubes 5 cm in diameter. This is a digital camera in which each of the PM tube outputs is individually digitized. (*Courtesy Dr. Joel Karp, University of Pennsylvania, Philadelphia, PA.*)

Many manufacturers employ plastic light guides between the detector crystal and PM tubes, whereas others couple the PM tubes directly to the crystal. The functions of the light guide are to increase the light collection efficiency, by channeling scintillation light away from the gaps between the PM tubes, and to improve the uniformity of light collection as a function of position. The latter effect is achieved by painting or etching a carefully designed pattern onto the entrance face of the light guide. The use of the PM tubes with hexagonal or square cross-sections that can be tiled without gaps on the NaI(Tl) crystal may in some cases allow elimination of the light guide, assuming there is sufficient spreading of the scintillation light in the glass entrance window of the PM tube for accurate positioning.

The detector crystal and PM tube array are enclosed in a light-tight, lead-lined protective housing. In most modern cameras, most of the electronics (such as preamplifiers, pulse-height analyzers, automatic gain control, pulse pile-up rejection circuits and ADCs) are mounted directly on the individual PM tube bases within the detector housing to minimize signal distortions that can occur in long cable runs between the detector head and control console.

The amount of light detected by a particular PM tube is inversely related to the lateral distance between the interaction site and the center of that PM tube. This is illustrated in one dimension in Figure 13-4. Ideally, the relationship between signal amplitude and location with respect to the center of a PM tube would be linear. This would enable the position of an event to be determined by taking a weighted average or centroid of the PM tube signals using the simple relationships shown in Figure 13-4. In practice, however, the response is more complex, with a plateau directly beneath the PM tube (because the PM tube is not a "point" detector) and long, flat tails caused by reflections of light from the back and side surfaces of the NaI(Tl) crystal. Therefore a calibration for spatial nonlinearity is required (see Chapter 14, Section B).

Figure 13-5A shows a schematic drawing for an eight-PM tube version of the gamma camera and is used to illustrate the principles of scintillation event localization in an *analog* detector. The position is determined by splitting the signal from each PM tube onto four output lines, whose signals are denoted X^+, X^-, Y^+, and Y^- (Fig. 13-5B). The fraction of the PM tube current that goes to each output line is determined by the value of the resistors

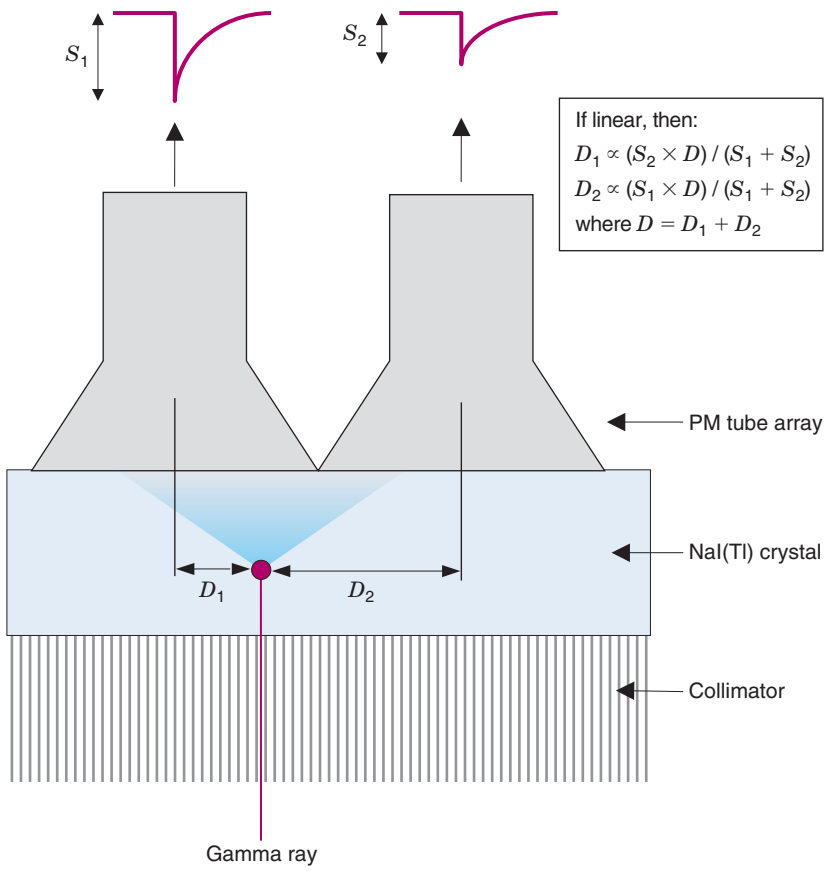

FIGURE 13-4 Illustration of light sharing between photomultiplier (PM) tubes. The PM-tube signal, *S,* is inversely related to the distance of the interaction site, *D,* from the center of the PM tube. Equations for a linear relationship are shown.

(R) that are used. By Ohm's law, this current is proportional to 1/R. A separate circuit sums the outputs of all the PM tubes to form the Z-signal. The Z-signal is proportional to the total amount of light produced by a scintillation event in the crystal, and therefore the total energy deposited by the gamma ray, and is used for pulse-height analysis.

The X^+, X^-, Y^+, and Y^- signals are combined to obtain *X-position* and *Y-position* signals. The *X*-position of the scintillation event is given by the difference in the X^+ and X^- signals, divided by the total *X* signal ($X^+ + X^-$)

$$X = (X^+ - X^-)/(X^+ + X^-) \qquad (13\text{-}1)$$

Similarly, for the *Y*-position

$$Y = (Y^+ - Y^-)/(Y^+ + Y^-) \qquad (13\text{-}2)$$

The *X*- and *Y*-position signals are normalized to the total *X* and *Y* signals, so that the calculated position of interaction does not depend on the pulse height. Note that the possible range of *X* and *Y* values is from –1 to +1. The resistor values shown in Figure 13-5C were chosen such that the calculated *X*- and *Y*-position signals vary linearly with distance in the X and Y directions. In a perfect gamma camera, measured (*X, Y*) values would change linearly from (–1, –1) in the bottom left-hand corner to (+1, +1) at the top right-hand corner of the camera face. The *X* and *Y* values can be scaled by the detector size to determine the absolute position of an event on the gamma camera face.

However, Equations 13-1 and 13-2 do not give a perfect mapping of source position because, as was discussed previously, the PM tubes signal does not actually vary linearly with interaction position. This gives rise to a "pincushion" artifact, which is illustrated in Figure 14-9. There are also effects caused by nonuniformities in the crystal, light reflections at the edge of the crystal, and nonuniform response across the face of the PM tubes that can cause further nonlinearities in

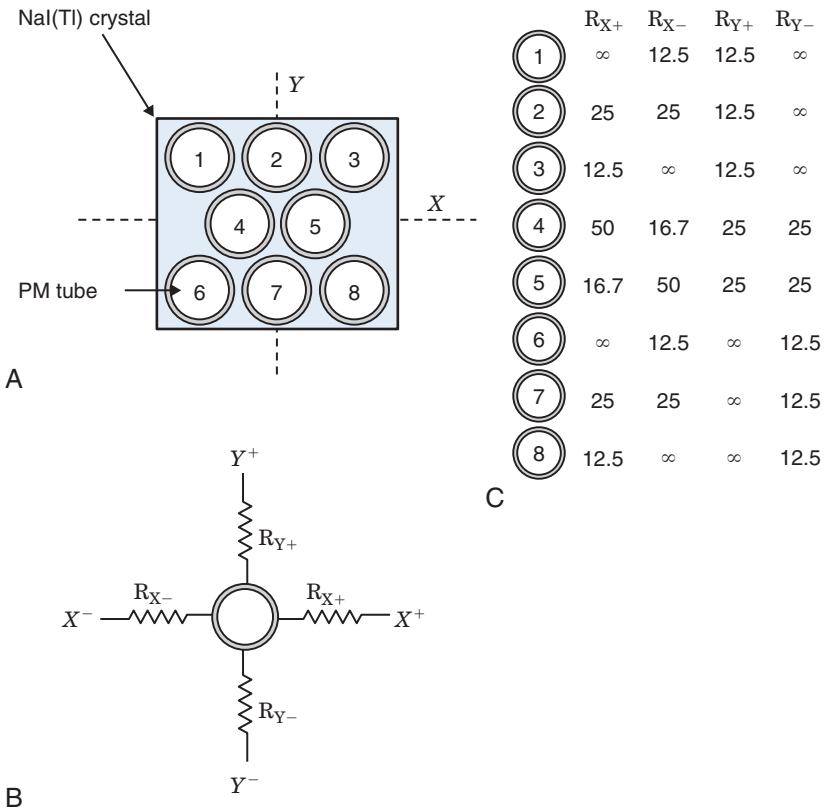

FIGURE 13-5 Illustration of analog positioning in a gamma camera. *A,* Schematic representation of an eight-photomultiplier (PM) tube camera. *B,* Signals from individual PM tubes are split using resistors onto four output lines, designated X^+, X^-, Y^+, and Y^-. *C,* Representative resistor values (in kΩ) for the eight PM tubes. Resistor values are chosen such that the X and Y positions computed from Equations 13-1 and 13-2 vary linearly with interaction position in the detector, ranging from a value of –1 in the bottom left hand corner to +1 in the top right corner.

position determination. These effects and correction techniques for them are discussed in Chapter 14, Section B.

In *digital* cameras, the output signal from each PM tube is digitized and the event position is calculated in software. Often, this is simply analogous to the resistor readout described earlier; the inverse of the resistor values are used as weighting factors for the individual PM tube signals, and Equations 13-1 and 13-2 are used to determine the X and Y values. However, digital cameras also can use more sophisticated algorithms that incorporate information regarding the nonlinearity of PM tube response with position into the weighting factors to provide better positioning accuracy.

A commonly used tactic that is employed in both digital and analog cameras to improve the positioning accuracy is to include in the position calculation only PM tubes with signals above a certain threshold. This has two important benefits. By using the signal only from those PM tubes that produce a significant pulse amplitude, the noise from the PM tubes that produce negligible signal amplitude (and that therefore contribute little to position information) is not included in the position calculation. Second, with signal thresholding, only a small number of PM tubes surrounding the interaction location are used for position determination. This allows a gamma camera to detect multiple events simultaneously when they occur in different portions of the gamma camera and their light cones (the projection of the scintillation light on the PM tube array) do not significantly overlap. This improves the counting rate performance of the gamma camera, reducing dead time losses.

Energy selection is important for imaging because it provides a means to discriminate against γ rays that been scattered within the body and therefore lost their positional information. By choosing a relatively narrow pulse-height analyzer window that is centered on the photopeak, only γ rays that undergo no scatter or small-angle scatter will be accepted.

Two different methods can be used to select the photopeak events. The first approach uses simple energy discrimination on the *Z*-signal. However, because of nonuniformities in the NaI(Tl) crystal (small variations in light production with position), in light collection efficiency and in PM tube gains, the position of the photopeak varies somewhat from position to position in the detector. If a single discriminator level is applied across the whole detector, the window must be widened to accommodate the fluctuations in photopeak position, thus accepting more scatter (Fig. 13-6, *top*).

In the second method, suitable only for digital cameras, the photopeak positions and appropriate discriminator level settings are computed and stored for many different locations across the detector face (Fig. 13-6, *bottom*). When an event is detected, the *X*, *Y* values are calculated based on Equations 13-1 and 13-2, and a look-up table is used to find the appropriate discriminator levels for that location. If the event amplitude *Z* falls within the pulse-height analyzer settings, the event is accepted.

A modern gamma camera has an energy resolution of 9% to 10% at 140 keV (^{99m}Tc). Typically, the *energy window* (the difference between upper-level and lower-level discriminators) is set to 14%, or 20 keV, centered around 140 keV. The gamma camera software adjusts the discriminator levels for radionuclides other than ^{99m}Tc based on the relationship (approximately linear over a small energy range) between the γ-ray energy deposited and the light output of NaI(Tl) (see Fig. 10-11).

3. Collimators

To obtain an image with a gamma camera, it is necessary to project γ rays from the source distribution onto the camera detector. Gamma rays cannot be focused; thus a "lens" principle similar to that used in photography cannot be applied. Therefore most practical γ-ray imaging systems employ the principle of *absorptive collimation* for image formation.* An absorptive collimator projects an image of the source distribution onto the detector by allowing only those γ rays traveling along certain directions to reach the detector.

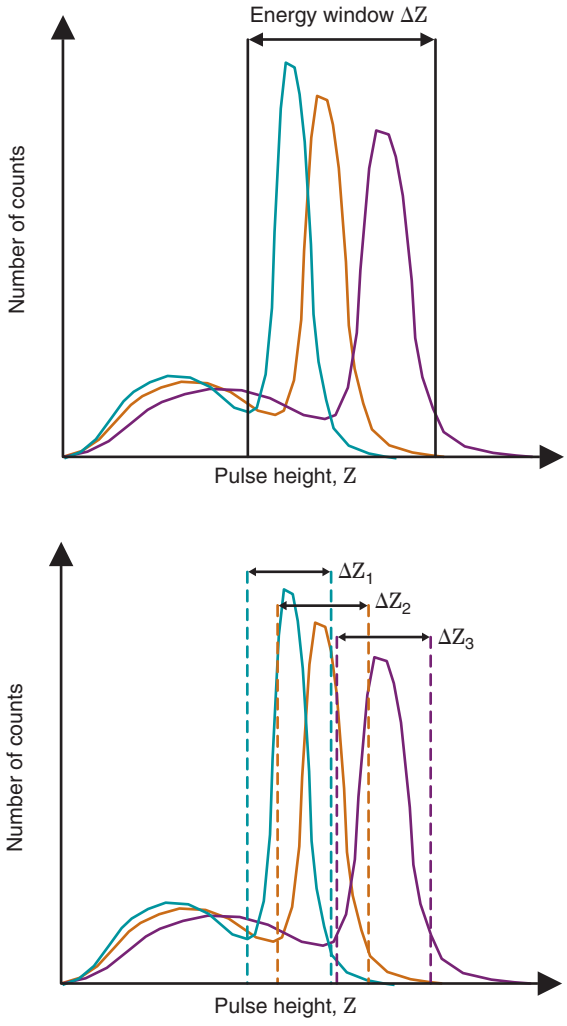

FIGURE 13-6 The pulse-height response is not uniform across the whole face of the gamma camera, leading to variation in the pulse height of photopeak events. Using a global energy window requires a wide window that leads to the inclusion of larger amounts of scatter and also results in nonuniform efficiency (*top*). Using local energy thresholds, in which the energy window is tailored to the event location, improves scatter rejection and uniformity (*bottom*).

Gamma rays not traveling in the proper direction are absorbed by the collimator before they reach the detector. This "projection by absorption" technique is an inherently inefficient method for using radiation because most of the potentially useful radiation traveling toward the detector actually is stopped by the absorptive walls between the collimator holes. This is one of the underlying reasons for the relatively poor quality of radionuclide images (e.g., as compared to radiographic images), as discussed in Chapter 15.

Four basic collimator types are used with the gamma camera: pinhole, parallel-hole,

*An important exception is imaging of the two 511-keV annihilation photons from positron-emitting radionuclides, in which electronic coincidence detection can be used to replace the collimator as described in Chapter 18, Section A.1.

diverging, and converging. The different types of collimator are introduced subsequently. Their effects on the spatial resolution and sensitivity of the gamma camera are discussed in Chapter 14 , Sections C and D.

A *pinhole* collimator (Fig. 13-7A) consists of a small pinhole aperture in a piece of lead, tungsten, platinum, or other heavy metal absorber. The pinhole aperture is located at the end of a lead cone, typically 20 to 25 cm from the detector. The size of the pinhole can be varied by using removable inserts and is typically a few millimeters in diameter.

The imaging principle of a pinhole collimator is the same as that employed with inexpensive "box cameras." Gamma rays passing through the pinhole project an inverted image of the source distribution onto the detector crystal. The image is magnified when the distance b from the source to the pinhole is smaller than the collimator cone length f; it is minified when the source distribution is farther away. The image size I and object (source) size O are related according to

$$I/O = f/b \tag{13-3}$$

The size of the imaged area also changes with distance from the pinhole collimator. If the detector diameter is D and the magnification (or minification) factor is I/O (Equation 13-3), the diameter of the image area projected onto the detector, D', is

$$D' = \frac{D}{I/O} \tag{13-4}$$

Thus a large magnification factor, obtained at close source-to-collimator distances, results in a small imaged area.

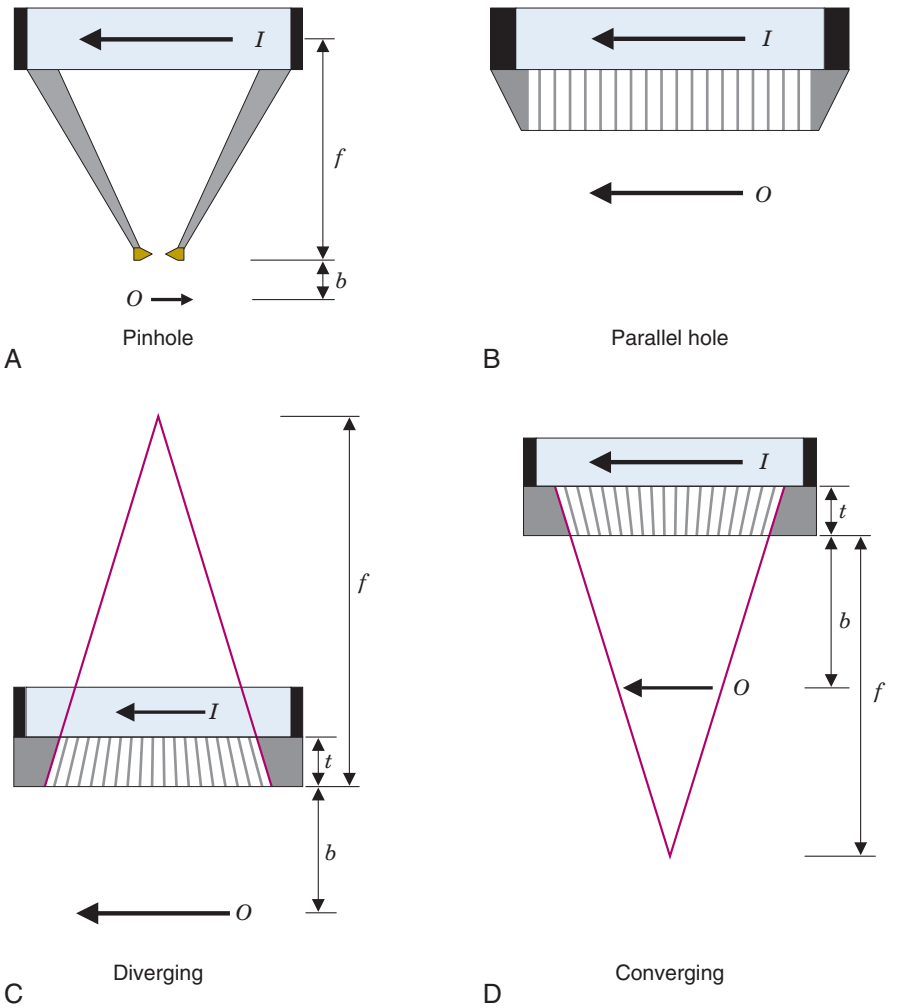

FIGURE 13-7 *A-D,* Four types of collimators used to project "γ-ray images" onto the detector of a gamma camera. *O,* Radioactive object; *I,* its projected image.

Image size changes with object-to-pinhole distance b. Therefore the pinhole collimator provides a somewhat distorted image of three-dimensional objects because source planes at different distances from the collimator are magnified by different amounts. Pinhole collimators are used primarily for magnification imaging of small organs (e.g., thyroid and heart) and for small-animal imaging.

Another type of pinhole collimator, the *multi-pinhole collimator,* has an array of multiple pinholes, typically seven, arranged in a hexagonal pattern. This collimator was employed in the past for tomographic imaging. This type of tomography now is seldom used clinically; however, multi-pinhole approaches are being widely employed for some small-animal imaging applications.

The *parallel-hole collimator* (Fig. 13-7B) is the "workhorse" collimator in most imaging laboratories. Parallel holes are drilled or cast in lead or are shaped from lead foils. The lead walls between the holes are called collimator *septa.* Septal thickness is chosen to prevent γ rays from crossing from one hole to the next (see Chapter 14, Section C.2). A magnified view of a parallel-hole collimator is shown in Figure 13-8. The parallel-hole collimator projects a γ-ray image of the same size as the source distribution onto the detector. A variation of the parallel-hole collimator is the slant-hole collimator, in which all of the holes are parallel to each other but angled, typically by approximately 25 degrees, from the perpendicular direction. This type of collimator has characteristics that are similar to those of the parallel-hole type. Because it views the source distribution from an angle rather than directly "head-on," it can be positioned closer to the patient for better image detail in some imaging studies (e.g., left anterior oblique cardiac views).

A *diverging collimator* (Fig. 13-7C) has holes that diverge from the detector face. The holes diverge from a point typically 40-50 cm behind the collimator, projecting a *minified,* noninverted image of the source distribution onto the detector. The degree of minification depends on the distance f from the front of the collimator to the convergence point, the distance b from the front of the collimator to the object (source), and the collimator thickness t

$$I/O = (f - t)/(f + b) \qquad (13\text{-}5)$$

where I and O are image and object size, respectively. The useful image area becomes larger as the image becomes more minified (Equation 13-4).

EXAMPLE 13-1

What is the minification factor for a diverging collimator 5-cm thick, with f = 45 cm, and a source distribution 15 cm from the collimator? If the detector diameter is 30 cm, what is the imaged area at this distance?

Answer

From Equation 13-5,

$$I/O\text{(minification factor)} = (45 - 5)/(45 + 15) = 0.67$$

From Equation 13-4,

$$\text{Diameter of imaged area} = 30\text{ cm}/0.67 = 44.8\text{ cm}$$

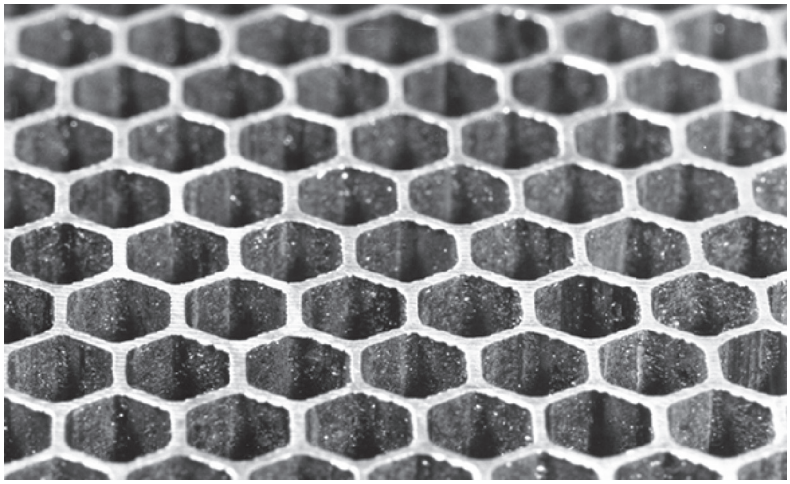

FIGURE 13-8 Close-up view of a typical parallel-hole collimator showing the hole structure. Individual holes are approximately 1.9 mm across in this example. (*Courtesy Nuclear Fields, Des Plaines, IL.*)

As shown by Example 13-1, a typical diverging collimator decreases the size of the image on the detector and increases the diameter of the imaged area, by approximately one-third as compared with a parallel-hole collimator. As with the pinhole collimator, image size changes with distance; thus there is a certain amount of image distortion. Diverging collimators are used primarily on cameras with smaller detectors to permit imaging of large organs such as the liver or lungs on a single view.

A *converging collimator* (Fig. 13-7D) has holes that converge to a point 40-50 cm in front of the collimator. For objects between the collimator face and the convergence point, the converging collimator projects a *magnified,* noninverted image of the source distribution. Image size I and object size O are related according to

$$I/O = (f + t)/(f - b) \qquad (13\text{-}6)$$

where f is the distance from the collimator face to the convergence point, b is the distance from the collimator face to the object, and t is collimator thickness.

Some manufacturers provide a single, invertible collimator insert that can be used in either converging or diverging mode.

EXAMPLE 13-2

Suppose the collimator described in Example 13-1 is inverted and used as a converging collimator to image a source distribution 15 cm in front of the collimator, also with a 30-cm diameter detector. What are the image magnification factor and the size of the imaged area?

Answer

When the collimator is inverted, the back face becomes the front face, and the convergence distance f becomes (45 – 5 cm) = 40 cm. Thus from Equation 13-6

$$I/O \text{ (magnification factor)} = (40 + 5)/(40 - 15) = 1.8$$

From Equation 13-4,

$$\text{Diameter of imaged area} = 30 \text{ cm}/1.8 = 16.7 \text{ cm}$$

Again, because magnification depends on distance, there is some image distortion with the converging collimator (Fig. 13-9). Converging collimators are used primarily with cameras having large-area detectors to permit full use of the available detector area for imaging of small organs.

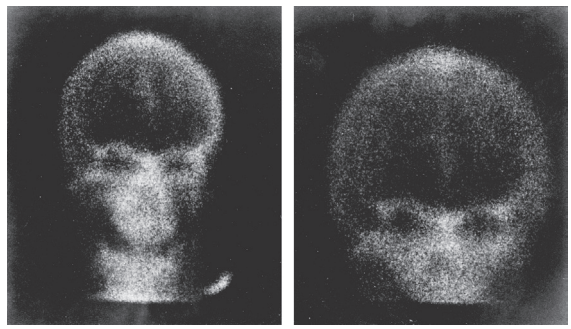

Parallel-hole collimator Converging collimator

FIGURE 13-9 Examples of geometric image distortions created by the converging collimator.

Converging collimators project an inverted *magnified* image when the object is located between the convergence point and twice the convergence length of the collimator, and an inverted *minified* image beyond that distance; however, they are used rarely at distances beyond the convergence point.

One consequence of the magnification or minification effects of these collimators is that the contribution of the intrinsic detector resolution (see Chapter 14, Section A) to the resulting image resolution may be reduced (magnification > 1) or increased (magnification < 1). Thus magnifying collimators can be useful in situations in which high spatial resolution is required, for instance in imaging of small organs such as the thyroid and in small-animal imaging applications.

4. Event Detection in a Gamma Camera

There are four types of events that may be detected by a gamma camera, as illustrated in Figure 13-10. Of these, only one provides correct positional information. The four events types (labeled to correspond with Fig. 13-10) are the following:

A: *valid event*—a γ ray is emitted parallel to the collimator holes, passes through a hole and interacts photoelectrically in the NaI(Tl) crystal, depositing all of its energy at a single location.

B: *detector scatter event*—a γ ray is emitted parallel to the collimator holes, passes through a hole and interacts by Compton scattering in the NaI(Tl) crystal. The scattered γ ray can either interact a

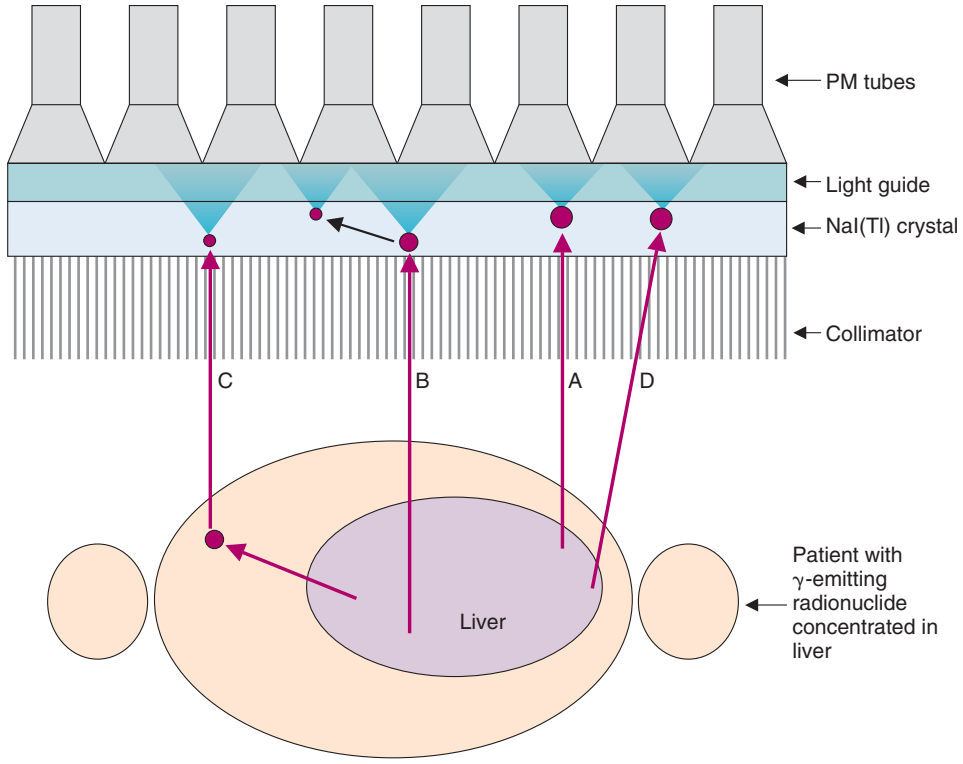

FIGURE 13-10 Illustration of different types of events that may be detected by a gamma camera. *Red circles* indicate locations of γ ray interactions. A, Valid event. B, Detector scatter event. C, Object scatter event. D, Septal penetration.

second time in the detector (as illustrated in Fig. 13-10), in which case the full energy of the γ ray is deposited, or it may escape the detector, in which case only part of the γ-ray energy is deposited. In the former case, energy discrimination cannot be used to reject the event, and the event will be mispositioned between the two interaction locations. In the latter case, it is likely that the event will be rejected because it does not satisfy the event energy criteria established by the upper- and lower-level discriminators. As discussed in Chapter 14, Section A.1, these events are relatively rare.

C: *object scatter event*—the γ ray is not emitted toward the collimator holes but is scattered within the body, then passes through a collimator hole and subsequently is detected. The γ ray loses energy during scattering and will therefore produce a smaller signal in the detector. Some of these events will be rejected by energy discrimination, but if the angle of scatter is small ($\lesssim$45 degrees), the energy loss is small and the event may be accepted. In this case the event is mispositioned, often many centimeters from the original site of emission. These events lead to a low-spatial-frequency background in the images that results in a loss of contrast. (See Chapter 15, Section C.). In clinical imaging situations, a large fraction of the detected events can be due to object scatter, and good energy resolution in the gamma camera is extremely important (see Chapter 14, Section A.3). The collimator itself can also be a cause of scatter leading to similar effects.

D: *septal penetration*—in this case a γ ray is emitted toward the collimator, but not parallel to it. Because of incomplete attenuation by the thin collimator walls (*septal penetration*), there is a finite chance that the γ ray will reach the NaI(Tl) crystal and interact with it. This again leads to blurring of the image, because all events are considered to have come from a direction perpendicular to the collimator face (for parallel-hole collimators). This effect becomes increasingly important when using high-energy γ emitters or high-resolution collimators with thin septa.

Considerable effort is expended in the design of gamma cameras to reduce or eliminate the detection of the events B, C, and D just described, each of which is a cause of blurring and a loss of contrast in the image. Collimators also are carefully designed for specific energies to minimize septal penetration while maximizing sensitivity for a given γ-ray energy (Chapter 14, Section C).

In addition to the simple cases illustrated in Figure 13-10, a combination of these event types can occur (e.g., scatter in the body and septal penetration, or septal penetration followed by Compton interaction in the detector). Finally, further complications arise when pulse pile-up occurs—that is, two or more events occur almost simultaneously in the gamma camera. This can also lead to event mispositioning and is discussed in detail in Chapter 14, Section A.4. Pile-up events can arise from of any combination of the event types described earlier.

C. TYPES OF GAMMA CAMERAS AND THEIR CLINICAL USES

The most common type of gamma camera is the *single-headed* system (Fig. 13-11). It consists of a gamma camera detector mounted on a gantry that allows the camera head to be positioned in a flexible way over different regions of the patient's body. Often, a moving bed is incorporated to permit imaging studies of the whole body. The gamma camera head often is mounted on a rotating gantry, allowing it to take multiple views around the patient. This feature also is necessary for producing *tomographic* images, or cross-sectional images through the body, as discussed in Chapters 16 and 17.

Dual-headed gamma cameras are becoming increasingly popular. In these systems, two gamma camera heads are mounted onto the gantry as shown in Figure 13-12. Usually, the two heads can be positioned at a variety of locations on the circular gantry. An obvious advantage of a dual-headed camera is that two different views of the patient can be acquired at the same time. For example, in whole-body imaging, the two detector heads can be placed at 180 degrees to each other to provide anterior and posterior views simultaneously. Triple-headed systems also exist, primarily for tomographic studies, as described in Chapters 16 and 17.

An example of a planar image acquired with a gamma camera system is presented in Figure 13-13. Dynamic processes can also be measured by taking multiple planar images

FIGURE 13-11 Single-headed gamma camera mounted on a rotating gantry. The camera is operated from the computer (*left*). The flexible positioning of the camera head and the bed (*right*) allows the system to obtain images of many different parts of the body. (*Courtesy GE Medical Systems, Milwaukee, WI.*)

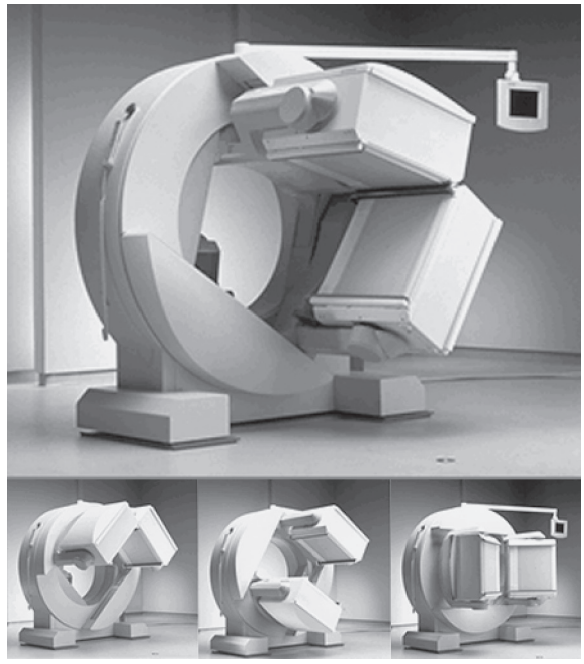

FIGURE 13-12 A dual-headed gamma camera system (*top*). Note that the camera heads can be placed in different orientations to provide two simultaneous views of an organ or the body (*bottom*). (*Courtesy Siemens Medical Systems, Inc., Hoffman Estates, IL.*)

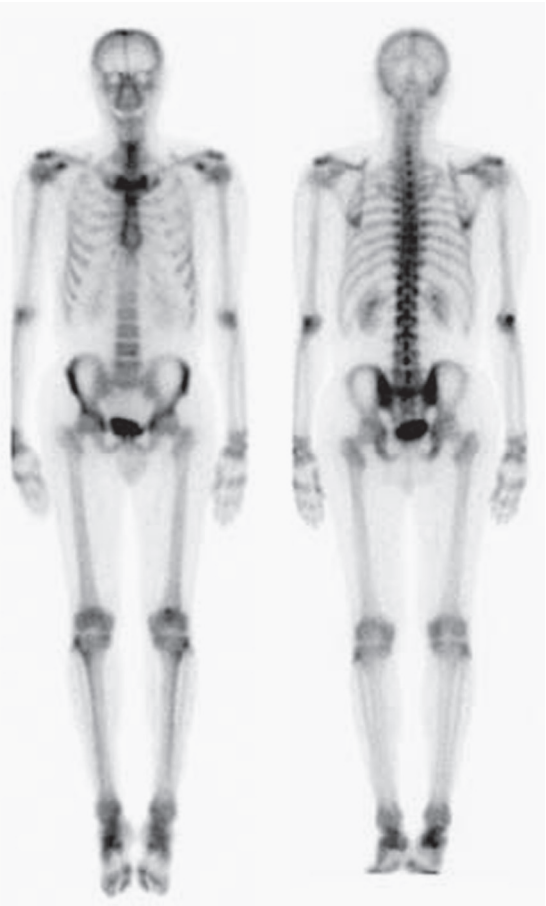

FIGURE 13-13 Whole-body bone scan obtained using ^{99m}Tc-MDP. These planar images were obtained with a dual-headed gamma camera on which both anterior (*left*) and posterior (*right*) views can be acquired simultaneously. The entire body was imaged by translating the patient bed through the gamma camera system. (*Courtesy Siemens Medical Systems, Inc., Hoffman Estates, IL.*)

over time. An example of a dynamic study is shown in Figure 13-14.

Single- and dual-headed gamma cameras are the workhorses of clinical nuclear medicine laboratories. However, a range of specialty gamma cameras have been or are being developed for specific imaging tasks. Examples are systems designed specifically for small-organ imaging (e.g., heart, breast, and thyroid) and mobile systems for use on patients who are too sick to be moved to the nuclear medicine department (e.g., from intensive care). These systems typically have smaller detector heads and may not have a built-in bed. An example of a compact gamma camera for breast imaging and representative images from it are shown in Figure 13-15. The detector typically ranges from 10×10 cm^2 to 20×20 cm^2. A number of different detector technologies are being exploited for these small-detector cameras, including traditional NaI(Tl)/PM tube systems, cameras based on pixellated NaI(Tl) or cesium iodide [CsI(Tl)] scintillator arrays (see Fig. 13-15B), and CsI(Tl) scintillator arrays with read-out by silicon photodiode arrays. There are also systems being developed that employ arrays of cadmium zinc telluride elements (see Chapter 7, Section B) for direct detection of γ rays, eliminating the need for a scintillator-photodetector combination.

High-resolution gamma cameras also have been developed for small-animal imaging. The goal is to provide a tool that biologists can use to monitor radiotracers in vivo, particularly in rats and mice. Most approaches involve the use of very small pinhole

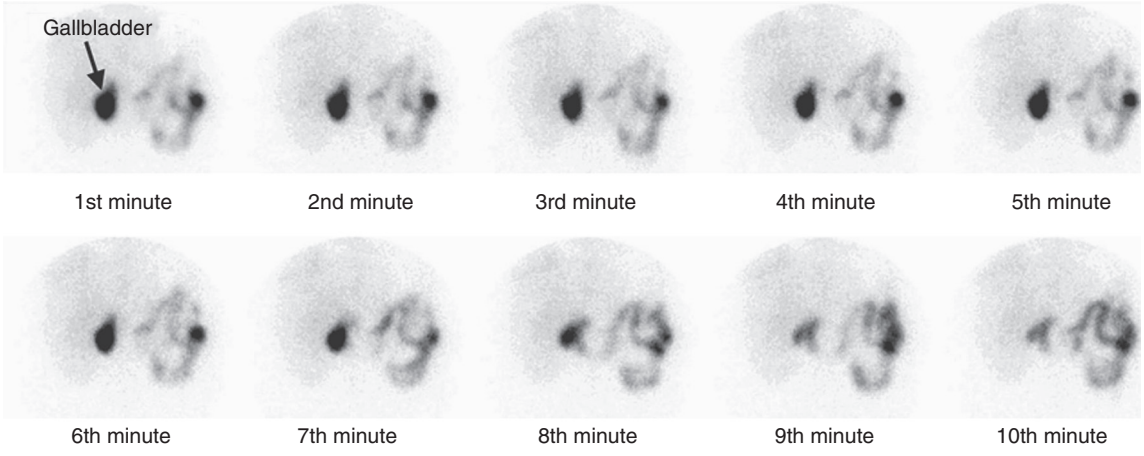

FIGURE 13-14 Planar gamma camera images over the region of the gallbladder following injection of ^{99m}Tc-HIDA. At approximately 7 minutes, cholecystokinin was given to the patient to stimulate emptying of the gallbladder. The rate and extent of emptying can be measured from this dynamic sequence of planar images. (*Courtesy GE Medical Systems, Milwaukee, WI.*)

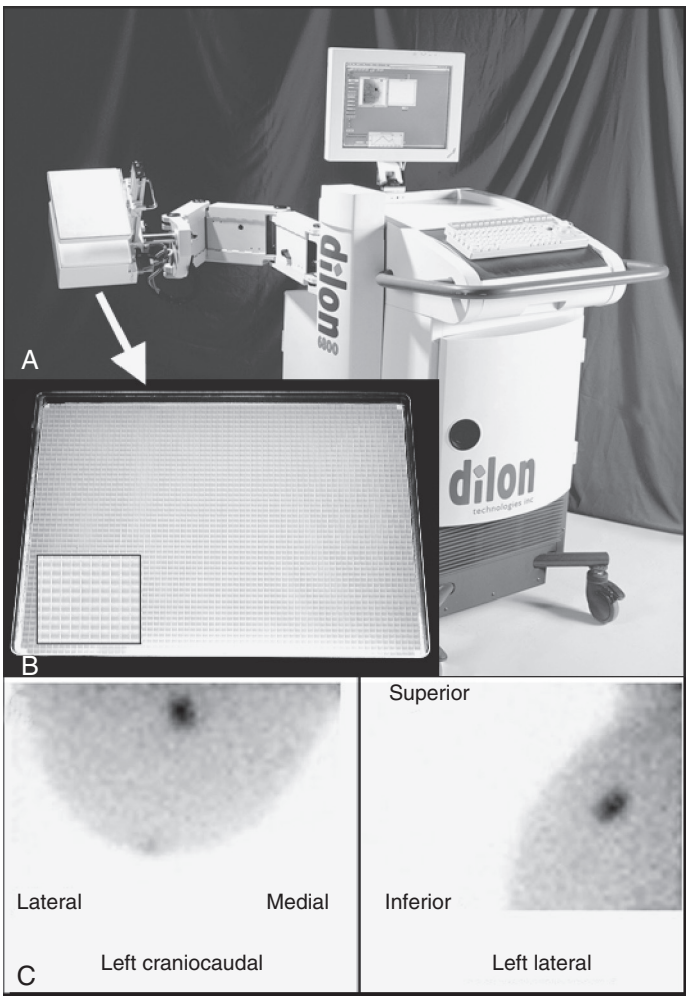

FIGURE 13-15 Example of a compact, mobile gamma camera system. *A,* The gamma camera head is attached to a cantilevered arm for easy and flexible positioning. *B,* Pixellated NaI(Tl) scintillator array that is coupled to small position-sensitive photomultiplier tubes to form the detector head. Each element in the array is approximately 2×2 mm and is separated from its neighbor by a reflective material. The *inset* shows a magnified view of the pixel elements. *C,* Clinical images of a breast cancer patient acquired with this camera following the injection of ^{99m}Tc-sestamibi. A tumor is seen as a "hot spot" against the low background uptake of the normal breast. (*Photographs and images courtesy Dilon Technologies, Inc., Annapolis, MD.*)

collimators to provide high spatial resolution. Tomographic small animal imaging systems based on this approach are discussed in Chapter 17, Section A.3.

REFERENCE

1. Anger HO: Scintillation camera. *Rev Sci Instr* 29:27-33, 1958.

BIBLIOGRAPHY

The principles of the gamma camera are discussed in greater detail in the following:

Simmons GH: *The Scintillation Camera*, New York, 1988, Society of Nuclear Medicine.